An improved model for remaining useful life prediction on capacity degradation and regeneration of lithium-ion battery

Li-Ming Deng[1], Yu-Cheng Hsu[2], and Han-Xiong Li[3]

[1,2,3] *City University of Hong Kong, Hong Kong, China*
limngdeng2-c@my.cityu.edu.hk
rayxx1234@gmail.com
mehxli@cityu.edu.hk

ABSTRACT

The regeneration phenomena of the lithium-ion battery are widely existed in reality but rarely studied due to the gap between experiment conditions and practical working conditions. In this paper, the capacity regeneration phenomena are considered during the degradation process of batteries. An improved empirical model incorporating both rest time and discharge cycles for remaining useful life (RUL) prediction is proposed. The degradation process and regeneration process have been described by different components and integrated to formulate the whole model. The dual estimation framework is employed to decouple the states and parameters during the degradation and regeneration process. The datasets from NASA Prognostics Center of Excellence (PCoE) have been adopted for model validation. The proposed model is compared with other empirical model and also different estimation methods. The results are satisfactory, and demonstrate the capability of the proposed model for the RUL prediction of Lithium-ion battery.

1. INTRODUCTION

Dramatic progresses have been made to put forward lithium-ion batteries as the main energy solution in many areas. Due to the performance of high energy density, high power density, and low weight, Lithium-ion batteries have replaced many other batteries in the market of computers, communications and other kinds of consumer electronics (He et al., 2011, Huggins, 2008, Nazri & Pistoia, 2008). The safety and security of batteries have been absorbed increasingly concerns accordingly. The failure of batteries could lead to loss of functions, millions of dollars or even human lives. The recent impact events are the series explosion of Galaxy Note 7, a kind of smartphones made by Samsung in 2016. Samsung had to recall the smartphones due to the failure of batteries, which

cost billions of dollars (Lopez, 2017). The reasons for the failure of batteries vary from design or manufacturing faults, aging, to unexpected operating conditions (Lawson, 2005). Battery aging is the process that battery performance gradually deteriorates with time due to the side reactions. The aging process is generally irreversible and eventually leads to the end of battery life, if not early ended by other reasons. The aging process can be characterized as the change of internal states, such as the decrease of capacity or the increase of internal impedance, over repeated charge and discharge cycles. When the internal states reach a specified threshold, the battery is generally considered to be unreliable. The remaining useful life (RUL) can be defined as the time span between the observation time and the time when the internal states reach the specified threshold (Xing et al., 2013, Yang et al., 2017).

Although the regeneration phenomenon has been mentioned by many studies (He et al., 2011, Qin et al., 2015), there are few studies on the regeneration phenomenon among the RUL or SOH prediction. Some detection methods for identifying the regeneration phenomenon have been conducted in literature. Oliveres et al. (Olivares et al., 2013) and Orchard et al. (M. E. Orchard et al., 2015) utilized regeneration detection modules, like PF-based detection module (M. E. Orchard & Vachtsevanos, 2009), RSPF-based detection module (M. Orchard et al., 2010) and their variants, to isolate the effects of capacity regeneration phenomenon and then incorporating the detection results into state space model for the end of life (EOL) prediction. Qin et al. (Qin et al., 2016) detected the regeneration phenomenon directly according to the difference between two adjacent cycles of the state of health (SOH), and then approximated the regeneration amplitude with a hyperbolic tangent function based on the rest period of time. However, all the aforementioned detection methods restrict the detection time of early detected regeneration phenomenon and inappropriate for multi-step-ahead prediction of RUL. Saha et al. (Saha & Goebel, 2009) regarded the regeneration phenomenon as self-recharge process and approximated it with an exponential model. Some researchers fol-

lowed this regeneration model (Jin et al., 2013, Tang et al., 2014) for RUL prediction. The exponential model has made some improvements for RUL prediction when the regeneration phenomenon appears.

Our paper focuses on the remaining useful life prediction under the consideration of the regeneration phenomenon. In section 2, the characteristics of degradation and regeneration process have been described and an improved empirical model has been developed for RUL prediction. The dual EKF has been introduced for parameter estimation in section 3. Section 4 presents the RUL prediction with the improved empirical model and the proposed estimation method. The detailed experiments and the results are described and compared in section 5 respectively. In section 6, we conclude our studies and also point out some problems in the proposed framework.

2. MODEL DEVELOPMENT

2.1. Capacity degradation and regeneration

The aging process of a lithium-ion battery includes the capacity degradation and regeneration. The degradation phenomenon is obvious that the capacity fades along with the repeated charge and discharge cycles. The regeneration phenomenon is defined as the battery capacity can be recovered partially during the process (Eddahech et al., 2013). As suggested in Figure 1, there are two main characteristics of the degradation and regeneration process:
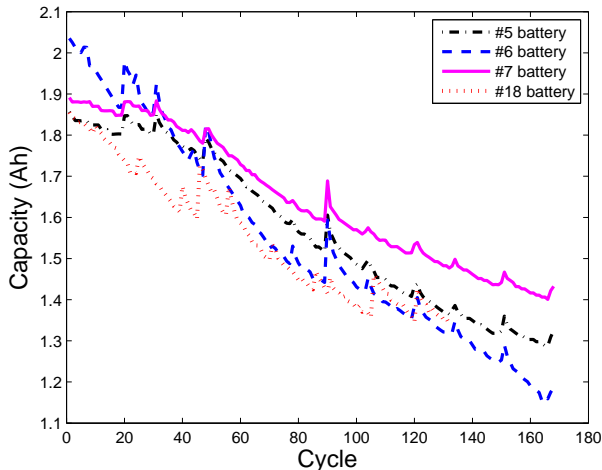

Figure 1. The degradation and regeneration process of 4 lithium-ion batteries.

- Capacity suffers sudden increments when the regeneration happens, and then degrades to the norm rate quickly (Olivares et al., 2013);
- The global capacity degradation rates are changeable,

and tends to be slow in total after considering the capacity rise due to the regeneration;

The capacity increments can extend the useful life of batteries. Failure of considering the regeneration phenomenon will be a great waste to early replace batteries before the useful life really ended.

2.2. Modeling capacity

The empirical model, introduced by Saha et al. (Saha & Goebel, 2009), combined the Coulombic efficiency as the capacity degradation rate, and the next cycle of charge capacity can be approximated by two components: one is the remaining capacity from the previous capacity degradation; the other is the capacity obtained from the regeneration during the rest. The model can be denoted as Equation (1).

$$C_{k+1} = \eta_C C_k + \beta_1 \exp(-\beta_2/\Delta t_k) \tag{1}$$

where η_C represents the Coulombic efficiency, C_k is capacity in cycle k, Δt_k indicates the rest time between cycle k and cycle $k + 1$, β_1 and β_2 are the model parameters. The Coulombic efficiency (η_C) is defined as the fraction of the prior charge capacity that is available during the following discharge (Huggins, 2008). Since the following available discharge capacity cannot be obtained in future cycles, the exact η_C is unavailable in the prediction stage. The decision of the η_C is quite an art and hard to be approximated because the Coulombic efficiency depends upon a number of factors and varied in each cycle. Thus, in previous studies, η_C is assumed as a fixed equivalent value on the whole.

As for the degradation of capacity during the aging process of lithium-ion batteries, the degradation rate varies according to the conditions of operation and the aging stage of batteries. The assumption that Coulombic efficiency is fixed in Equation (1) is inappropriate during the aging process. This motivates us allowing the parameter to be adjustable. To improve the adaptive capability of the model in Equation 1, we relax the fixed Coulombic efficiency η_C and estimate it with measured data. The proposed model is shown in Equation (2).

$$C_{k+1} = \alpha C_k + \beta_1 \exp(-\beta_2/\Delta t_k) \tag{2}$$

The notations are the same as the previous equation except the α that we regard it as a model parameter. However, the parameter and capacity are coupled together and each can be difficult to estimate. The dual estimation framework is employed to decouple their interactions. The detailed methods will be presented in the next section.

3. DUAL EXTENDED KALMAN FILTER

3.1. State-space model

State space model originates from control engineering for describing a system in terms of inputs, outputs, and states in

vector space (Wan & Van Der Merwe, 2000). We denote the states x_k and the observations y_k at the time k. In Kalman filter, the assumption is that states follow first order Markov process, which means that current states are conditionally independent to all previous states except those states right before the current states (Haug, 2012, Welch & Bishop, 1995).

$$p(x_k|x_{k-1}, x_{k-2}, ..., x_0) = p(x_k|x_{k-1}) \qquad (3)$$

The model used in Kalman filter thus can be expressed by

$$x_k = f(x_{k-1}, w_{k-1}) \qquad (4)$$

$$z_k = h(x_k, v_k) \qquad (5)$$

where f and h are the transformation function of the process and measurement. w_k and v_k are the process noise and measurement noise in the model.
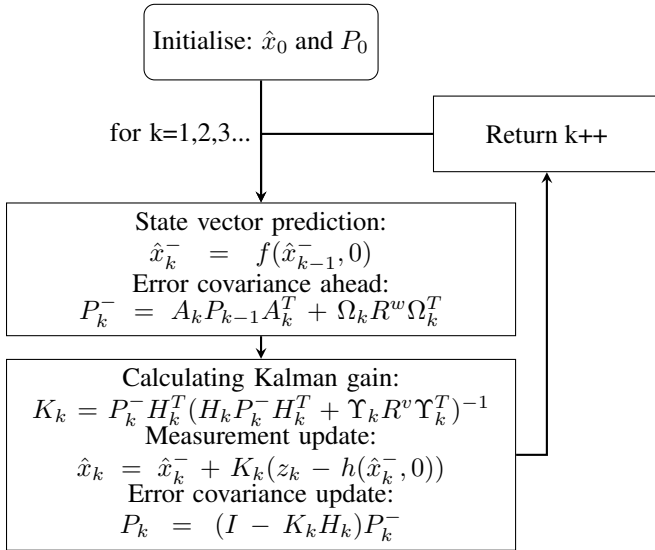

Figure 2. Flowchart for extended Kalman filter estimation.

3.2. Extended Kalman filter

Kalman filter is developed to resolve the discrete-data filtering problem by minimizing the mean-square-error of a state-space model (Wan & Van Der Merwe, 2000, Welch & Bishop, 1995, Haug, 2012). Many researchers used Kalman filter and its family to model battery degradation (Lu et al., 2013).

When Kalman filter was first introduced, it can only solve the linear system. Over years of development, extended Kalman filter was developed to approximately solve the non-linear filtering problem (Welch & Bishop, 1995).

In the process, we assume that w_k and v_k are white noise follow the Gaussian distribution with the covariance R^w and R^v. The non-linear transformation may distort white noise which no longer follows the normal distribution. As a result, the ex-

tended Kalman filter (EKF) is an estimator for the nonlinear system (Welch & Bishop, 1995).

The idea of EKF is using the first order Tylor expansion to approximate the non-linear system (Haug, 2012). The approximation equations are formulated as Equation (6) and (7).

$$x_k \approx \tilde{x}_k + A(x_{k-1} - \hat{x}_{k-1}) + \Omega w_{k-1} \qquad (6)$$

$$z_k \approx \tilde{z}_k + H(\hat{x}_k - x_k) + \Upsilon v_k \qquad (7)$$

where A and Ω are the partial derivative of f with respect to x and w respectively. Likewise, H and Υ are the partial derivative of h with respect to x and v. The implementation(Najim, 2010, Haug, 2012) detail is shown in Figure 2.
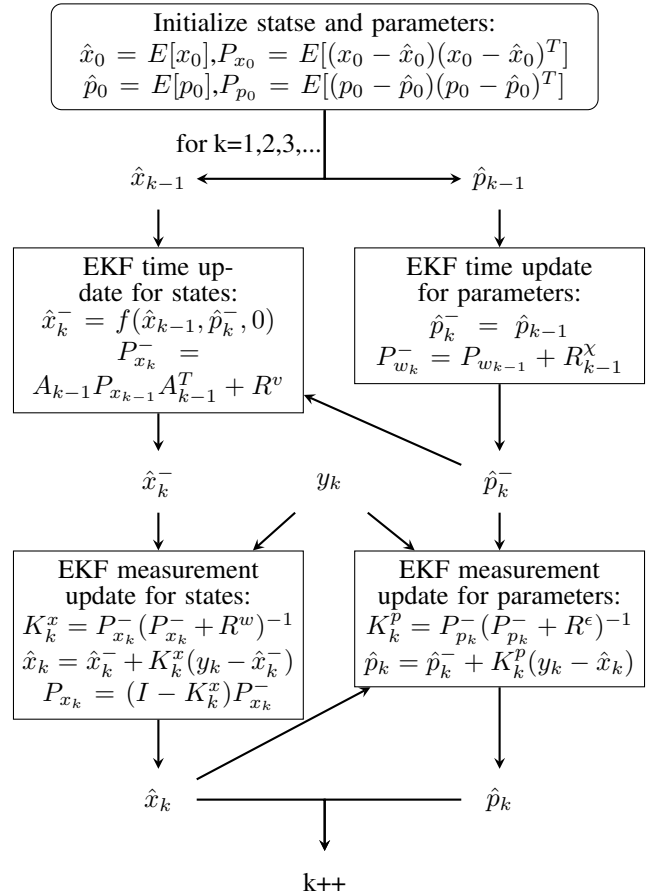

Figure 3. Flowchart for dual extended Kalman filter estimation.

3.3. Dual estimation

In the remaining useful life prediction of batteries, the clean state is not available and coupled with parameters in the empirical model. To decouple the states and parameters, the dual extended Kalman filter which employs an extended Kalman filter tracking on state variables and the other ex-

tended Kalman filter tracking parameters of the process (Wan & Nelson, 2001).

Given that we have a series of states and outputs $[x_k, d_k]$, we can use extended Kalman filter to estimate the parameter of the process p_k at time step k (Wan & Nelson, 2001). Because the parameter ideally should remain same value, the parameters state-space model are written as

$$p_{k+1} = p_k + \chi_k \qquad (8)$$

$$d_k = h(x_k, \chi_k) + \epsilon_k \qquad (9)$$

where χ_k is the noise during the process with covariance R^χ, h is the observation function, and ϵ_k is the measurement error. Therefore, we can apply extended Kalman filter government parameter estimation(Wan & Nelson, 2001).

In the dual extended Kalman filter, we consider the situation that we estimate not only parameters but also the hidden process states by extended Kalman filter. In particular, the EFK calculation in battery remaining useful life estimation is easier as the state x_k and the output y_k are the same (i.e. capacity of battery). Therefore, $z_k = h(x_k, v_k) = Ix_k + v_k$ The implementation framework (Wan & Nelson, 2001, Plett, 2004, 2005) is shown in Figure 3.

4. REMAINING USEFUL LIFE PREDICTION

In this section, we reformulate the model in Equation (2) with state-space model. The transition model of parameters is defined as Equation (10), the state (capacity) transition model is shown in Equation (11).

$$p_{k+1} = \begin{bmatrix} \beta_{1,k+1} \\ \beta_{2,k+1} \\ \alpha_{k+1} \end{bmatrix} = \begin{bmatrix} \beta_{1,k} \\ \beta_{2,k} \\ \alpha_k \end{bmatrix} + \begin{bmatrix} \chi_1 \\ \chi_2 \\ \chi_3 \end{bmatrix} \begin{matrix} \chi_1 \sim N(0, \sigma_1^2) \\ , \chi_2 \sim N(0, \sigma_2^2) \\ \chi_3 \sim N(0, \sigma_3^2) \end{matrix} \quad (10)$$

where the noise χ follows the gaussian distribution, with zero mean and σ^2 variance.

$$C_{k+1} = \alpha_k C_k + \beta_{1,k} \exp(-\beta_{2,k}/\Delta t_k) + \chi_4, \\ \chi_4 \sim N(0, \sigma_4^2) \qquad (11)$$

The capacity is selected as the measurement output, and the measurement error is selected as Gaussian noise, as shown in Equation (12)

$$z_k = C_k + v_k, \\ v_k \sim N(0, \sigma_5^2) \qquad (12)$$

With the measurement capacity and the obtained rest time, the dual extended Kalman filtering method is then incorporated to update the parameters and the state capacity. On the prediction stage, the parameters and the state are updated sequentially according to the transition model. The prediction of capacity is thus obtained after the state has been updated. The predicted RUL is then extracted from the predicted ca-

pacity that first hit the specified threshold, as shown in Equation (13)

$$RUL = k_{te} - k_{t0} \qquad (13)$$

where k_{t0} is the end of cycle that the measurement capacity updated via the Equation (12), which means the training of the model is finished and starts for the prediction. k_{te} is the cycle that the predicted capacity hits the specified threshold for the first time, that is $C_{k_{te}} \leq C_{threshold} < C_{k_{te}-1}$.
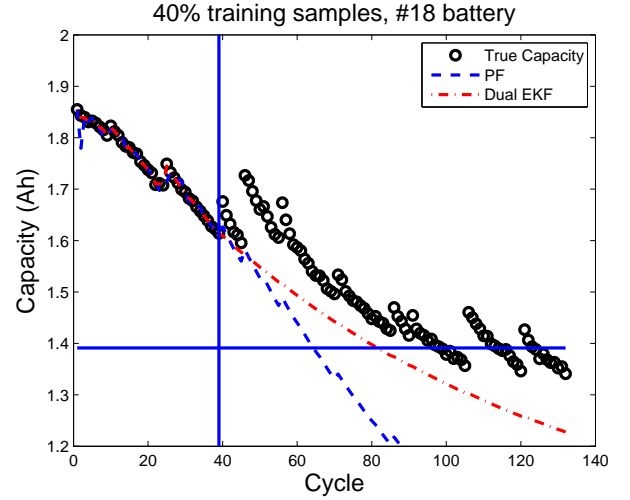
(a) Model B estimated with joint PF and dual EKF
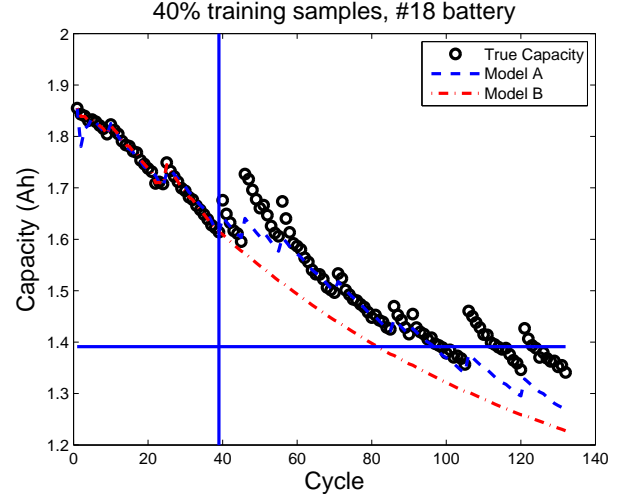
(b) Model A estimated with PF and model B estimated with dual EKF

Figure 4. Comparison of RUL prediction results under 40% training samples of # 18 battery.

5. EXPERIMENTS AND RESULTS

The battery datasets from NASA Prognostics Center of Excellence (PCoE) (Saha & Goebel, 2007) have been adopted in this study. Three different operational profiles (charge, discharge, and impedance) have been sequentially committed for

Table 1. COMPARING THE PERFORMANCE OF RUL PREDICTION

| Battery N.o.	True RUL	Model A based PF		Model B based PF		Model B based dual EKF	
		Prediction	Absolute error	Prediction	Absolute error	Prediction	Absolute error
B0005	98 (%60 of AL)	-[a]	-	22	76	90	8
	65 (%40 of AL)	45	20	51	14	61	4
	33 (%20 of AL)	15	18	10	23	28	5
B0006	62 (%60 of AL)	101	49	37	25	63	1
	41 (%40 of AL)	37	4	19	22	41	0
	21 (%20 of AL)	15	6	6	21	16	5
B0007	96 (%60 of AL)	64	32	36	60	77	19
	64 (%40 of AL)	37	27	14	50	52	12
	32 (%20 of AL)	14	18	8	24	27	5
B0018	60 (%60 of AL)	59	1	27	33	44	16
	40 (%40 of AL)	45	5	12	28	38	2
	20 (%20 of AL)	12	8	5	15	16	4

[a]The RUL prediction failed.
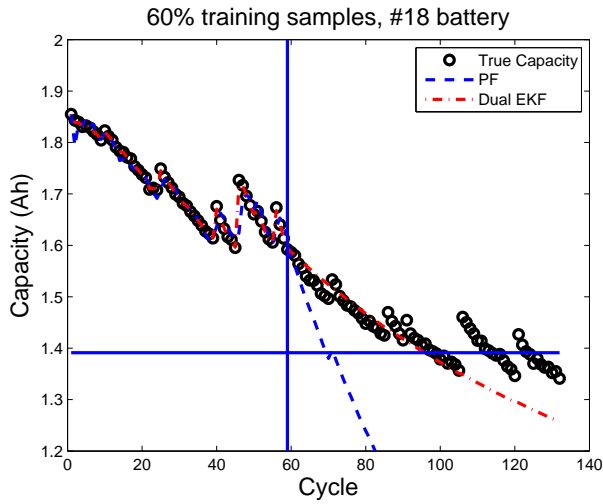
(a) Model B estimated with joint PF and dual EKF
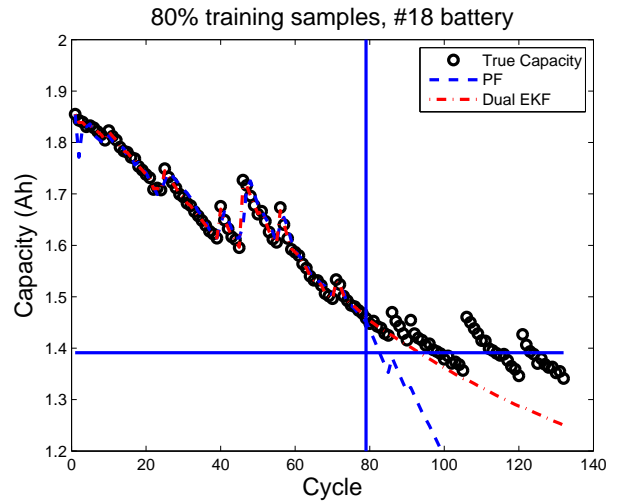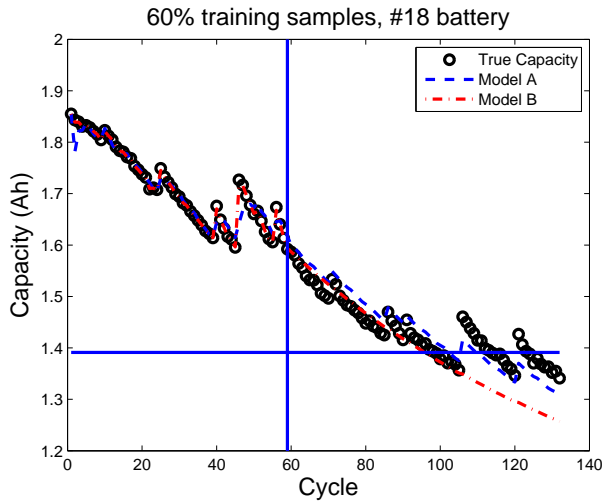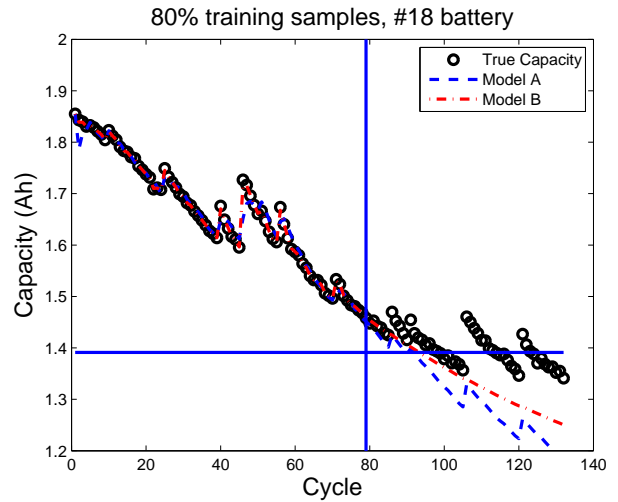
(b) Model A estimated with PF and model B estimated with dual EKF

Figure 5. Comparison of RUL prediction results under 60% training samples of # 18 battery.

(a) Model B estimated with joint PF and dual EKF

(b) Model A estimated with PF and model B estimated with dual EKF

Figure 6. Comparison of RUL prediction results under 80% training samples of # 18 battery.

four Li-ion batteries (# 5, 6, 7 and 18) at room temperature, and repeated until their capacity faded 30%.

To investigate the effective of our proposed framework, we compare the RUL prediction performance among the improved model estimated with dual EKF and joint particle filtering, and also the original model (Saha & Goebel, 2009) estimated with particle filtering. In the setting of our experiments, the actual life (AL) is defined as the cycle duration that the capacity fades 30% for # 5 and # 6 batteries. Since the capacity when fades 30% of the beginning capacity is smaller than all the extracted capacity from # 7 and # 18 battery dataset, AL for these two batteries is calculated according to a 25% fades of capacity in order to utilize the datasets. The RUL is defined as the number of cycles from current cycle to the cycle that the capacity fades to the aforementioned indicators. In order to investigate the prediction performance of the models on different degradation phases, models are trained with 40%, 60% and 80% of AL data respectively, and RUL is predicted based on the trained models accordingly. Thus, the true RUL is the remaining life cycles given the current trained AL, that are 60%, 40% and 20% of AL data accordingly. The true RUL, the prediction results and the absolute prediction errors are summarized in Table 1. Where Model A represents the original model as shown in Equation (1) and Model B represents our improved model as shown in Equation (2). The estimation methods are also indicated in the table.

Our proposed framework, Model B estimated by dual EKF method, outperform the other paradigms in RUL prediction on most of the degradation phases for all batteries. Here, we visualize the tracking and prediction capacity for # 18 battery on different prediction start cycles, as shown in Figure 4, Figure 5 and Figure 6 respectively. The plots for other batteries have similar properties and are not displayed here. The vertical blue line in each figure represents the end of the training samples, in other words, the start cycle for the prediction of capacity. The horizontal blue line in each figure represents the specified threshold to decide the end of life for batteries. Then, the prediction RUL can be visualized as the cycle length from the start prediction cycle (vertical blue line) to the corresponding cycle that the prediction capacity hits the horizontal blue line (capacity threshold).

The sub-figure in Figure 4(a), Figure 5(a) and Figure 6(a) are comparing the parameter estimation methods between the joint particle filtering and the dual EKF for our proposed model. All these sub figures demonstrate that the joint particle filtering underestimated the future capacity. A possible reason may be the state capacity and the degradation rate α coupled together and will be adjusted as a whole αC_k. If the degradation rate α is adjusted with some errors, the errors may be compensated by adjusting the state capacity simultaneously. Thus, there is no guarantee for accurate estimation of α. Although the dual estimation cannot capture the regeneration obviously, the prediction lines are bent up, which alleviate the underestimation of future capacity. From the sub-figure in Figure 4(b), Figure 5(b) and Figure 6(b), these figures compare the prediction performance of original model (Model A) and the improved model (Model B). From each figure, it is obvious that the predicted capacity obtained from model A is roughly a straight line though some sudden rise in the regeneration area. However, the degradation trend of battery capacity will not always be a straight line. Thus, an adjustable degradation rate in our improved model is more accurate for the prediction of future capacity.

Only one case that the Model A with less absolute error than Model B, as also shown in Figure 4(b). This happens accidentally when the fixed degradation rate η_C is roughly equal to the future overall degradation rate. However, finding the specified degradation rate η_C is very difficult, which relates to the degradation profile, prediction start cycles and the end of life. Thus, the results demonstrate the capability and superior of our proposed model and the dual EKF estimation method for RUL prediction under regeneration phenomenon.

6. CONCLUSION

In this paper, an improved empirical model has been proposed and analyzed for RUL prediction under regeneration phenomenon. The proposed model inherently demonstrates the superiority for RUL prediction due to the adjustable parameter can approximate the changeable degradation rate reasonably. The dual EKF estimation has been employed to deal with the coupled problem of parameter and state. The exponential term can improve the prediction accuracy further for considering the influence of the regeneration phenomenon. The prediction performance of the proposed framework has been validated by the lithium-ion battery datasets from PCoE. The results are favorable comparing to other methods. However, the sudden rise capacity during the regeneration is not predicted obviously as other methods. There is still some room for the improvements of this proposed framework. Further work is to consider the real working conditions as suggested in (Daigle & Kulkarni, 2016).

REFERENCES

Daigle, M., & Kulkarni, C. S. (2016). End-of-discharge and end-of-life prediction in lithium-ion batteries with electrochemistry-based aging models.

Eddahech, A., Briat, O., & Vinassa, J.-M. (2013). Lithium-ion battery performance improvement based on capacity recovery exploitation. *Electrochimica Acta*, *114*, 750–757.

Haug, A. J. (2012). *Bayesian estimation and tracking: a practical guide*. John Wiley & Sons.

He, W., Williard, N., Osterman, M., & Pecht, M. (2011).

Prognostics of lithium-ion batteries based on dempster–shafer theory and the bayesian monte carlo method. *Journal of Power Sources*, *196*(23), 10314–10321.

Huggins, R. (2008). *Advanced batteries: materials science aspects*. Springer Science & Business Media.

Jin, G., Matthews, D. E., & Zhou, Z. (2013). A bayesian framework for on-line degradation assessment and residual life prediction of secondary batteries inspacecraft. *Reliability Engineering & System Safety*, *113*, 7–20.

Lawson, B. (2005). *Why batteries fail.* http://www.mpoweruk.com/failure_modes.htm. (Accessed: 2017-05-26)

Lopez, M. (2017). *Samsung explains note 7 battery explosions, and turns crisis into opportunity.* https://www.forbes.com/sites/maribellopez/2017/01/22/samsung-reveals-cause-of-note-7-issue-turns-crisis-into-opportunity/#743f1f9b24f1. (Accessed: 2017-05-26)

Lu, L., Han, X., Li, J., Hua, J., & Ouyang, M. (2013). A review on the key issues for lithium-ion battery management in electric vehicles. *Journal of power sources*, *226*, 272–288.

Najim, M. (2010). *Modeling, estimation and optimal filtration in signal processing* (Vol. 25). John Wiley & Sons.

Nazri, G.-A., & Pistoia, G. (2008). *Lithium batteries: science and technology*. Springer Science & Business Media.

Olivares, B. E., Munoz, M. A. C., Orchard, M. E., & Silva, J. F. (2013). Particle-filtering-based prognosis framework for energy storage devices with a statistical characterization of state-of-health regeneration phenomena. *IEEE Transactions on Instrumentation and Measurement*, *62*(2), 364–376.

Orchard, M., Tang, L., Saha, B., Goebel, K., & Vachtsevanos, G. (2010). Risk-sensitive particle-filtering-based prognosis framework for estimation of remaining useful life in energy storage devices. *Studies in Informatics and Control*, *19*(3), 209–218.

Orchard, M. E., Lacalle, M. S., Olivares, B. E., Silva, J. F., Palma-Behnke, R., Estévez, P. A., ... Cortés-Carmona, M. (2015). Information-theoretic measures and sequential monte carlo methods for detection of regeneration phenomena in the degradation of lithium-ion battery cells. *IEEE Transactions on Reliability*, *64*(2), 701–709.

Orchard, M. E., & Vachtsevanos, G. J. (2009). A particle-filtering approach for on-line fault diagnosis and failure prognosis. *Transactions of the Institute of Measurement and Control*, *31*(3-4), 221–246.

Plett, G. L. (2004). Extended kalman filtering for battery management systems of lipb-based hev battery packs: Part 3. state and parameter estimation. *Journal of Power sources*, *134*(2), 277–292.

Plett, G. L. (2005). Dual and joint ekf for simultaneous soc and soh estimation. In *Cd-rom proceedings of the 21st electric vehicle symposium (evs21),(monaco: April 2005).*

Qin, T., Zeng, S., & Guo, J. (2015). Robust prognostics for state of health estimation of lithium-ion batteries based on an improved pso–svr model. *Microelectronics Reliability*, *55*(9), 1280–1284.

Qin, T., Zeng, S., Guo, J., & Skaf, Z. (2016). A rest time-based prognostic framework for state of health estimation of lithium-ion batteries with regeneration phenomena. *Energies*, *9*(11), 896.

Saha, B., & Goebel, K. (2007). *Battery data set.* https://ti.arc.nasa.gov/tech/dash/pcoe/prognostic-data-repository/#battery. (Accessed: 2016-05-03)

Saha, B., & Goebel, K. (2009). Modeling li-ion battery capacity depletion in a particle filtering framework. In *Proceedings of the annual conference of the prognostics and health management society* (pp. 2909–2924).

Tang, S., Yu, C., Wang, X., Guo, X., & Si, X. (2014). Remaining useful life prediction of lithium-ion batteries based on the wiener process with measurement error. *Energies*, *7*(2), 520–547.

Wan, E. A., & Nelson, A. T. (2001). Dual extended kalman filter methods. *Kalman filtering and neural networks*, 123–173.

Wan, E. A., & Van Der Merwe, R. (2000). The unscented kalman filter for nonlinear estimation. In *Adaptive systems for signal processing, communications, and control symposium 2000. as-spcc. the ieee 2000* (pp. 153–158).

Welch, G., & Bishop, G. (1995). An introduction to the kalman filter.

Xing, Y., Ma, E. W., Tsui, K.-L., & Pecht, M. (2013). An ensemble model for predicting the remaining useful performance of lithium-ion batteries. *Microelectronics Reliability*, *53*(6), 811–820.

Yang, F., Wang, D., Xing, Y., & Tsui, K.-L. (2017). Prognostics of L i(NiMnCo)O2-based lithium-ion batteries using a novel battery degradation model. *Microelectronics Reliability*, *70*, 70–78.